

# Predicting respiratory motion for real-time tumour tracking in radiotherapy

Tomas Krilavičius<sup>a,b,\*</sup>, Indrė Žliobaitė<sup>c,a</sup>, Henrikas Simonavičius<sup>d</sup>, Laimonas Jaruševičius<sup>e</sup>

<sup>a</sup>*Baltic Institute of Advanced Technology, Saulėtekio 15, LT 10224, Vilnius, Lithuania*

<sup>b</sup>*Vytautas Magnus University, Vileikos 8, LT 44404, Kaunas, Lithuania*

<sup>c</sup>*Dept. of Computer Science, Aalto University, P.O. Box 15400, FI-00076 Aalto, Finland*

<sup>d</sup>*Rubedo Systems, UAB, Jovary 2, LT 47193, Kaunas, Lithuania*

<sup>e</sup>*Hospital of Lithuanian University of Health Sciences Kauno Klinikos, Eivenių g. 2, LT 50009, Kaunas, Lithuania*

---

## Abstract

*Purpose.* Radiation therapy is a local treatment aimed at cells in and around a tumor. The goal of this study is to develop an algorithmic solution for predicting the position of a target in 3D in real time, aiming for the short fixed calibration time for each patient at the beginning of the procedure. Accurate predictions of lung tumor motion are expected to improve the precision of radiation treatment by controlling the position of a couch or a beam in order to compensate for respiratory motion during radiation treatment.

*Methods.* For developing the algorithmic solution, data mining techniques are used. A model form from the family of exponential smoothing is assumed, and the model parameters are fitted by minimizing the absolute disposition error, and the fluctuations of the prediction signal (jitter). The predictive performance is evaluated retrospectively on clinical datasets capturing different behavior (being quiet, talking, laughing), and validated in real-time on a prototype system with respiratory motion imitation.

*Results.* An algorithmic solution for respiratory motion prediction (called EXSMI) is designed. EXSMI achieves good accuracy of prediction (error 4 – 9 mm/s)

---

\*Corresponding author

*Email addresses:* [t.krilavicius@bpti.lt](mailto:t.krilavicius@bpti.lt) (Tomas Krilavičius), [indre.zliobaite@aalto.fi](mailto:indre.zliobaite@aalto.fi) (Indrė Žliobaitė), [henrikas.simonavicius@rubedo.lt](mailto:henrikas.simonavicius@rubedo.lt) (Henrikas Simonavičius), [laimonas.jarusevicius@kaunoklinikos.lt](mailto:laimonas.jarusevicius@kaunoklinikos.lt) (Laimonas Jaruševičius)

with acceptable jitter values (5–7 mm/s), as tested on out-of-sample data. The datasets, the code for algorithms and the experiments are openly available for research purposes on a dedicated website.

*Conclusions.* The developed algorithmic solution performs well to be prototyped and deployed in applications of radiotherapy.

*Keywords:* Respiratory motion compensation, exponential smoothing, predictive modeling, real-time

---

## 1. Introduction

The goal of radiotherapy treatment is to destroy the tumor and at the same time prevent the healthy surrounding tissues from being damaged [1, 2, 3, 4, 5]. Advances in radiotherapy technologies, such as *intensity modulated or image guided radiotherapy*, and *stereotactic body radiotherapy*, have made highly conformal and accurate treatment [6] possible. An important limiting factor to the success of tightly conforming dose distributions is the ability to aim the radiation beam precisely at the target with minimal positional error.

Therefore, motion management is one of the most active research and development topics in modern radiotherapy, as can be seen from many studies [2, 7, 8, 9, 10].

*Intrafraction motion* (motion of the target during treatment) is usually caused by the skeletal muscular, cardiac, gastrointestinal and respiratory systems, the later being responsible for the most of it.

The positions of all the organs in the thorax and abdominal regions are affected by respiration of a patient; however, the organs may move in different ways and various magnitude. In addition, the tumor itself may be moving along with the organs, depending on its location and fixation to the surrounding structures. The magnitude of the motion highly depends on the location of the tumor and also may vary a lot for individual patients. *Lung tumors* can exhibit up to 3 cm motion in the cranio-caudal direction during normal respiration, while tumors of other types typically move only a few millimeters or do not move

at all [11]. Movement of lung tumors introduces uncertainty in the positioning. To account for this uncertainty the conventional radiation therapy requires larger treatment margins, as it is recommended by the International Commission on Radiation Units and Measurements [12, 13]. Extra margins may lead to large volumes of healthy tissue being destroyed during radiotherapy treatments. Therefore, while higher doses of radiation therapy may improve survival rate, healthy tissue sparing is important to reduce side effects of the organs at risk. [2].

To cope with this problem various techniques have been considered [2]. Active motion compensation [1, 14], such as *gated radiotherapy* [15, 16], *breath-hold* [17] or *tumor tracking* [18, 19, 20, 7] have been introduced into the clinical practice. However, these techniques have limitations, e.g., the total treatment time significantly increases in case of gated radiotherapy [21], invasive fiducial markers need to be implanted [22], breath-hold works well only in case of compliant patient. Hence, development of new non-invasive techniques, aimed to controlling respiratory motion in radiotherapy, is an important task for the modern radiation oncology. Some tracking systems, such as VERO [23], that use a beam for positioning and some, like CyberKnife [24] use robotic arm to move linac.

A generic approach to the compensation for respiratory motion is defined as follows (following [1]): (i) determine the current position of the tumor from an external marker position using a computational technique for relating the marker and the tumor [1, 5, 25, 26]; (ii) predict the next position of the tumor; (iii) compensate for the anticipated respiratory motion (e.g. by repositioning the beam); and (iv) adapt the dosimetry to the changing configuration of the tumor. The current position of a tumor can be determined using external markers [26, 3, 25, 5]. Once the next position of the tumor is predicted, various techniques can be used to compensate for the respiratory motion [27, 2, 1], e.g. shifting the patient using a robotic-couch, shifting the beam by repositioning the radiation source, redirecting the beam electromagnetically, or changing the aperture of the beam.

This study focuses on step (ii), i.e., predicting the next position of the tumor from the past observations. Prediction is necessary to overcome delays introduced by tracking system latency. For predicting the tumor motion a number of predictive modeling techniques have been considered [1, 14, 2], such as: Kalman filters [3, 1, 28], artificial neural networks (ANN) [3, 29], state-based probabilistic approaches [20], local regression[19], seasonal autoregressive models (TVSAR) [30], autoregressive moving average models (ARMA) [31], multi-step linear methods (MULIN) [32], and wavelet-based multiscale autoregression (wLMS) [33].

While most of the existing studies propose new advanced predictive models, the complete compensation process itself is understudied. After selecting an accurate predictive modeling technique, it is far from trivial to put it in operation, for which a full algorithmic solution is required. Algorithmic solutions should include step-by-step instructions for automated data pre-processing, model calibration for a given patient, adaptation to potential variation in data arrival rates, confidence estimation and self-diagnosing mechanisms of the model, and potential mode switching (e.g., to a simpler model or no prediction at all). The calibration procedure should be done as efficiently as possible in order to minimize preparation time, and maximize utilization of the equipment for treatment.

This paper proposes a full algorithmic solution for respiratory motion prediction for a selected setup (see sec. 2.1), aiming at minimizing the time for model calibration. The predictive performance is evaluated on clinical datasets off-line and in real-time on prototype system with respiratory motion imitation.

Several studies develop controllers for motion compensation [34, 35], which can be seen as algorithmic solutions, however, their focus is on step (iii), i.e. compensating for the anticipated respiratory motion, in Murphy’s classification, while our focus is on step (ii), i.e. predicting the next position of the tumor.

The remainder of the paper is organized as follows. Sect. 2 discusses data collection (2.1), prediction setting (2.2), performance criteria (2.3), prediction methods (2.4), algorithmic solution (2.5) and experimental evaluation (2.6). In Section 3 the performance of the algorithm is evaluated, and in Section 4

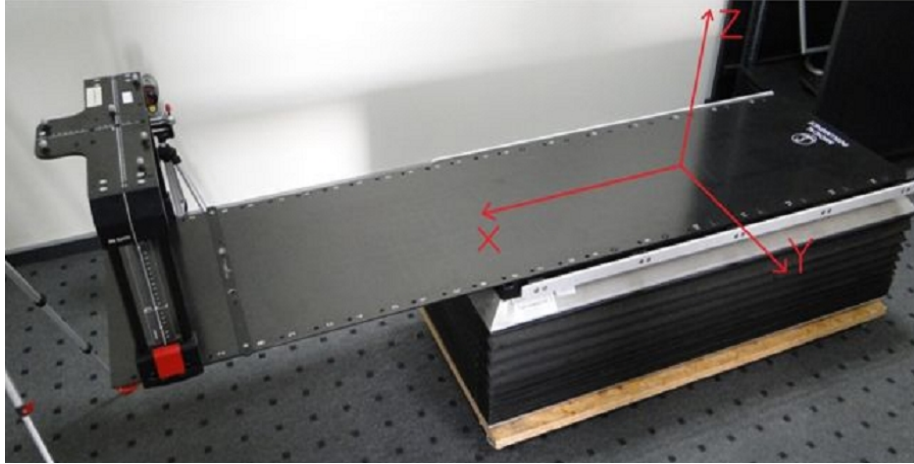


Figure 1: General setup for data collection.

experimental results are discussed. Conclusions and future research directions are presented in Section 5.

## 2. Materials and Methods

### 2.1. Data Collection

Clinical data is collected using an infrared stereo-camera with 60 Hz internal sampling frequency, external markers, HexaPOD evo couch and in-house software. Elekta HexaPOD<sup>TM</sup> evo RT System<sup>1</sup> (Elekta AB, Stockholm Sweden) is a radiation therapy system setup, with static positioning system iGuide®2.0 developed by Rubedo Systems<sup>2</sup> (Rubedo Systems, Kaunas, Lithuania). The system was adapted to collect real-time data by Rubedo Systems.

The radiation treatment system under consideration consists of several components: *patient setup couch*, in this case the HexaPOD couch<sup>3</sup> [36], *radiation*

---

<sup>1</sup><http://www.elekta.com/healthcare-professionals/products/elekta-oncology/treatment-techniques/positioning-and-immobilization/hexapod-evo-rt-system.html>

<sup>2</sup><http://rubedo.lt/>

<sup>3</sup>[http://www.elekta.com/assets/Elekta-Oncology/Stereotactic-Radiation-Therapy/case\\_studies/](http://www.elekta.com/assets/Elekta-Oncology/Stereotactic-Radiation-Therapy/case_studies/)

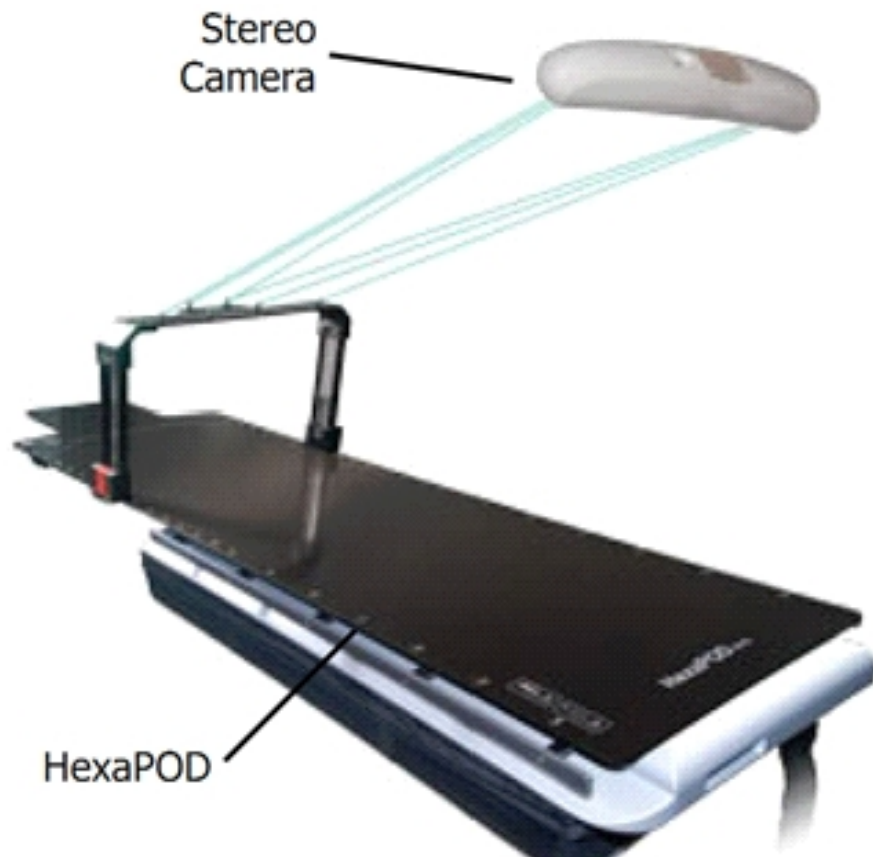


Figure 2: Camera position for data collection.

*beam source*, usually a *medical linear accelerator (linac)*, *tracking device*, which provides information about the position of the patient and a *controller* that controls the treatment process. Several different control schemes have been proposed [37, 38, 39, 27, 7].

Respiratory motion in HexaPOD is measured by an infrared stereo-camera (NDI Polaris [40] (NDI (Northern Digital) International, Ontario, Canada)), that tracks external markers placed on the body of the patient. We use 1 mm spatial resolution, and while the camera can provide up-to 0.25 mm resolution under ideal conditions [40], often it may go up-to 0.6 mm (with 95% confidence

interval), therefore 1 mm is the safe choice<sup>4</sup>. The camera provides position data periodically in frames (and frame numbers). The timestamps are computed from the sampling frequency of the internal camera, which is  $60Hz$  (a frame in each 16.7 ms). Processing delays are negligible ( $< 1$  ms).

The existing setup (provided by Rubedo systems) is restricted to processing every second (2nd) frame, therefore the effective sampling rate is 33.(3), 66.(6) or 100 (99.(9)) ms. See general setup and schematic camera position in Figs. 1 and 2 (this setup is used for the development and testing of iGuide software<sup>5</sup>). As a result, the raw incoming data is not completely equally spaced in time, i.e. the time intervals from the second to the sixth or the ninth frame may differ. We ensure that the data for prediction is equally spaced by resampling the incoming data at a rate that is a multiplier of six frames (which correspond to 100 ms). Due to the same reason, the prediction horizon should also be a multiplier of six frames. Prediction horizon is selected based on the specifics of setup, where we have 100 ms camera communication delay, and we predict future position 100 ms ahead to compensate velocity of the couch (16 mm/s).

Ten clinical datasets are used in this study. Each dataset includes 3-dimensional observation records with 3 positions per record over time. Each dataset records an empty treatment session (no radiation) lasting from 72.617 to 320.05 s. The datasets have been collected from 3 healthy males aged 20 to 40. See Table 1 for further information about the dataset.

## 2.2. Prediction task

Given is a three-dimensional time series recording the position of an external marker over time. The position is given in three coordinates  $x$ ,  $y$  and  $z$  in millimeters transformed in such a way that  $\min(x_i) = 0, \min(y_i) = 0$  and  $\min(z_i) = 0$ . Let  $r_i = (x_i, y_i, z_i)$  denote the *true position* of a marker at time  $i$ , and let  $\hat{r}_i^h = (\hat{x}_i^h, \hat{y}_i^h, \hat{z}_i^h)$  denote the *predicted position*  $h$  steps ahead. When the

---

<sup>4</sup>In case of 4 – 6 mm it could be insufficient.

<sup>5</sup>See <https://www.youtube.com/watch?v=a4Fqgl6avtA>.

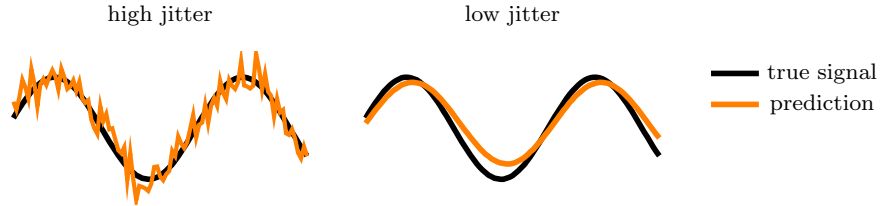


Figure 3: Two predictions giving the same prediction error but different jitters.

horizon  $h$  is clear from the context, it will be omitted from the notation. For brevity we index time series by the index of arrival and not by the time-stamp of arrival. The index  $i$  refers to the number of the current observation in a sequence from the start of the reading on the current patient.

### 2.3. Performance criteria

From the operational point of view two performance characteristics are critical: predictions should be accurate and the predicted signal should fluctuate as little as possible (have low jitter [14]). The latter requirement is due to the need for the beamer or the couch to move, following the predicted signal, in order to compensate respiratory motion. Following sudden rapid movements of predictions is impractical and may be infeasible due to mechanical limitations of couch or another tracking device. Fig. 3 gives two example predictions that lead to the same prediction error, but have different jitters. A low jitter is preferred from the operational point of view.

Quantitatively the accuracy of predictions can be measured by a straight line distance from the predicted position to the true position in 3-dimensional space (3D). For simplicity, distances can be measured in the coordinate units, but for interpretability it is better to transform the coordinates and report results in standard units of length. This paper reports prediction errors and jitters in millimeters. The prediction error at time  $i$  is defined as:

$$e_i = \sqrt{(x_i - \hat{x}_i)^2 + (y_i - \hat{y}_i)^2 + (z_i - \hat{z}_i)^2} = \|r_i - \hat{r}_i\|. \quad (1)$$

The goal is to minimize the error over a treatment session. Since treatment sessions can be of different length, it is practical to look at the mean error over



a treatment session:

$$E = \sum_{i=1}^T e_i / (T\Delta), \quad (2)$$

where  $T$  is the duration of the session in number of frames, and  $\Delta$  is the time interval between two frames.

The jumpiness or jitter [14] can be measured as the distance the prediction signal travels per time step:

$$\begin{aligned} j_i &= \sqrt{(\hat{x}_i - \hat{x}_{i-1})^2 + (\hat{y}_i - \hat{y}_{i-1})^2 + (\hat{z}_i - \hat{z}_{i-1})^2} \\ &= \|\hat{r}_i - \hat{r}_{i-1}\|. \end{aligned} \quad (3)$$

For the units (mm) to be interpretable and comparable to the error, in the experiments we will report average jitter and average error per second ( $\Delta = 0.1$ ).

The goal is to minimize jitter over a treatment session. Since treatment sessions can be of different length, it is practical to look at the mean jitter over a treatment session:

$$J = \sum_{i=2}^T j_i / ((T-1)\Delta), \quad (4)$$

where  $T$  is the duration of the session in number of frames, and  $\Delta$  is the time interval between two frames.

Note that jitter is minimized when  $\hat{r}_i = \hat{r}_{i-1}$  for all  $i \in [2, T]$ , i.e. the prediction is constant. However, in this case no compensation for respiratory movement is possible. In practice, a system aims at compensating for respiratory movement, it needs to find a balance between error and jitter.

#### 2.4. Predictive modeling techniques

We are aiming at developing an algorithmic procedure for real time prediction of respiratory motion. Such an algorithm takes a base model as input, and determines when the model should be calibrated, when the actual operation can start, and how to switch between alternative models of different complexity.

For predicting the tumor motion a range of predictive models have been considered [1, 14, 2], as discussed in the introduction. Our main qualitative criteria for choosing an existing technique for the algorithm are as follows.

1. Models need to be fast to calibrate (up to 30 – 60 sec) for every next patient, since waiting time is costly. The number of model design and calibration parameters should be minimal.
2. Models should be able to adapt to changes in respiration rhythm and drifts of the tumor during a session.
3. Models and prediction decisions should be transparent (how predictions are made), so that the technique can be trusted by medical specialists.
4. Models which are simple to implement on any treatment hardware with minimal usage of external tools are preferable to minimize risks of software errors and dependencies.

Table 2 provides a summary of considered base models and our assessment against the four qualitative criteria. The main limitation of state probabilistic methods (such as Kalman filters or Hidden Markov models) and autoregressive models (such as autoregressive moving average models, regression models fitted using least squares procedure) is that they require relatively large training sample for model calibration before it can be used for predictions, and we are looking for very fast and robust models. More advanced machine learning models (such as neural networks or support vector machines) require even larger training sample sizes, and in addition, the resulting models are so called "black box" models, where it is extremely difficult to trace how the predictions are made. Therefore, given the focus of our study on fast, interpretable, adaptive and transparent prediction making, we resort to extrapolation and exponential smoothing techniques for our algorithmic solution. The next subsections discuss these two types of techniques in detail.

#### *2.4.1. Extrapolation methods*

*Extrapolation methods.* predict based on the most recent observations. They do not require any calibration and minimum or none parameter settings. These methods have very short memory of the past data and hence are inherently adaptive to changes in respiration rhythm or tumor drifts, they are very transparent (easy to explain to a non-specialist) and very simple to implement.

*Persistent prediction.* (PP) is the simplest predictor, which predicts that the next signal will be the same as the last observed. No parameters are required.

$$\hat{x}_{t+h} = x_t, \quad (5)$$

here  $t$  is the time index and  $h$  is the prediction horizon.

Persistent prediction can be considered as a baseline for compensation for respiratory motion. It does not predict pro-actively, but only follows past observations.

*Linear extrapolation.* (LE) assumes that the signal will maintain the same velocity and direction as last observed. No parameters are required.

$$\hat{x}_{t+h} = x_t + (x_t - x_{t-h}). \quad (6)$$

*Multi-step linear prediction* (MULIN) [32] is a generalization over linear extrapolation, it takes into account acceleration of the signal of different order. Since the extrapolations may become unstable if the signal is noisy, MULIN uses exponential smoothing moving average of the predictions instead of outputting only the latest prediction.

$$\hat{x}_{t+h} = \alpha \left( x_t + \sum_{i=1}^k \delta(x_t, h)^i \right) + (1 - \alpha) \hat{x}_{t+h-1} \quad (7)$$

$$\delta(x_t, h)^1 = x_t - x_{t-h} \quad (8)$$

$$\delta(x_t, h)^{i+1} = \delta(x_t, h)^i - \delta(x_{t-h}, h)^i \quad (9)$$

where  $k \in [1, 2, \dots]$  and  $\alpha \in (0, 1)$  are user specified parameters. In this paper we experiment with the second order MULIN. We used the default parameter settings supplied in the implementation made available by the authors<sup>6</sup>.

#### 2.4.2. Exponential smoothing

*Exponential smoothing* is a type of moving average, where the importance of the past observations decreases exponentially. Exponential smoothing is not

---

<sup>6</sup><http://www.rob.uni-luebeck.de/~ernst/dateien/mulin/mulin.m>

parameter intensive, the only parameter is the speed with which old observations are forgotten. Exponential smoothing does not require model calibration for every new patient, it can predict immediately after the start, but a short warm-up period is advisable. Just like extrapolation methods, exponential smoothing is inherently adaptive, similarly transparent, and straightforward to implement.

*Simple exponential smoothing.* (ES1) makes prediction as the exponentially weighted moving average of the previous observations.

$$\hat{x}_{t+h} = \alpha x_t + (1 - \alpha)\hat{x}_{t-1}, \quad (10)$$

for any horizon  $h$ . Here  $\alpha \in (0, 1)$  is a user defined parameter. If the forgetting factor  $\alpha$  is small, then forecasting will have a long memory. If  $\alpha$  is close to one, then forgetting will be fast.  $\alpha = 1$  would mean that we predict the next observation to be the same as the last (PP).  $\alpha = 0$  would give a constant prediction (zero jitter). ES1 is equivalent to autoregressive integrated moving average model [41] ARIMA(0,1,1).

Simple exponential smoothing does not do well when there is a trend in the data.

*Double exponential smoothing.* (ES2) takes trends into account.

$$\hat{x}_{t+h} = l_t + hb_t \quad (11)$$

$$l_t = \alpha x_t + (1 - \alpha)(l_{t-1} + b_{t-1}) \quad (12)$$

$$b_t = \beta(l_t - l_{t-1}) + (1 - \beta)b_{t-1} \quad (13)$$

Here  $\alpha \in (0, 1)$  and  $\beta \in (0, 1)$  are user specified parameters. Initialization:  $l_0 = x_0, b_0 = 0$ . ES2 is equivalent to ARIMA(0,2,2).

In case of double exponential smoothing for respiratory motion prediction breath cycle will be modeled as short term trends.

The main limitation of this approach is that the prediction will systematically overshoot when the direction of the signal reverses.

*Holt-Winters exponential smoothing.* , or triple exponential smoothing (ES3), is often used for short term forecasting of seasonal time series [42], as it can handle trends and seasonality. Seasonality means that the signal is periodic with a period  $p$ . We consider ES3 model with additive seasonality component (based on [43]).

$$\hat{x}_{t+h} = l_t + hb_t + s_{t-p+h} \quad (14)$$

$$l_t = \alpha(x_t - s_{t-p}) + (1 - \alpha)(l_{t-1} + b_{t-1}) \quad (15)$$

$$b_t = \beta(l_t - l_{t-1}) + (1 - \beta)b_{t-1} \quad (16)$$

$$s_t = \gamma(x_t - l_{t-1} - b_{t-1}) + (1 - \gamma)s_{t-p} \quad (17)$$

Here  $\alpha \in (0, 1)$ ,  $\beta \in (0, 1)$  and  $\gamma \in (0, 1)$  are user specified parameters. Initialization:  $l_0 = x_0$ ,  $b_0 = 0$ ,  $s_0, \dots, s_{t-p} = 1$ .

The original ES3 requires the period to be known and fixed during the model operation. The period of a respiratory signal, however, varies even for a single patient, as respiration may become more frequent or slow down over time, the air intake may be delayed due to talking or coughing. We make a stabilizing modification to ES3, we use the initial level in estimation of the seasonal component instead of moving average of the level:

$$s_t = \gamma(x_t - l_0) + (1 - \gamma)s_{t-p}. \quad (18)$$

We suggest using the parameter values listed in Table 3, which have been found during initial experiments on the training parts of a couple of traces. The testing part of the traces on which the accuracies are reported, was never used for estimating these parameters. To minimize the chance of overfitting the training data the parameters are fixed for all the traces.

We suggest using a fast forgetting for the level (having in mind potential bias of the model and potential drifts), keeping it within a recommended [43] restriction  $0 < \alpha + \gamma < 1$ . The role of the trend component is to estimate long term changes in the average signal level, thus the memory should be long, thus for ES3  $\beta$  should be low. Since ES2 has no seasonal component, the trend

component plays the role of seasonal adjustment, thus  $\beta$  needs to be higher than in ES3, but not too high, since in such a case overshooting at turning points may be too large. Since we know that ES2 is biased (data contains seasonality, but we approximate it by the trend component), we need to have a fast forgetting not to propagate model bias therefore  $\alpha$  should be high.

### 2.5. Prediction procedure EXSMI

We propose the following procedure for predicting respiratory motion, called EXSMI, summarized in Algorithm 1. EXSMI includes online preprocessing outlier removal<sup>7</sup> (condition on line 9), online model calibration and switch prediction phase (line 11), a switching mechanism between the main model and a simple, but more robust baseline (line 18), which is based on the most recent performance, taking into account two quantitative criteria - prediction error and jitter (line 18). Linear extrapolation method is considered as a baseline  $B$ , and exponential smoothing is considered as the main predictive model ( $L$ ).

At the time of model switch (line 18) both models are well warmed up, and estimates of the most recent performance are available. We select the model demonstrating the lowest *recent* prediction error and jitter of the two and apply a fading factor  $\alpha$  to the running estimates of the performance to ensure that the most recent performance is accounted with more weight, while considering not-so-recent performance history with lower weight. IT helps to minimize the risk of sudden jumps in prediction error or jitter, when the predictors are switched. In the next section we experimentally analyze the performance of the proposed approach.

A recent study [44] aims at classifying the patients into predictable and unpredictable, in order to decide whether motion compensation should be used at all, which is conceptually similar to our approach, but there are several key differences. While the authors consider whether motion compensation should

---

<sup>7</sup>The threshold has been selected based on speed of the coach movement. It is not possible that the couch moves that fast as to produce 1 cm difference between points.

be used or not, we do not question the applicability of motion compensation, but dynamically switch between models of different complexity depending on the noisiness of the signal. Moreover, their approach is to decide regarding each patient before commencing the treatment, while our approach is intended for real time, and the outcome during each new treatment session may be different.

### *2.6. Protocol for experimental analysis*

We experimentally analyze the performance of the base models selected in Section 2.4 and the proposed algorithmic solution in the following settings. New observations arrive every 100 ms and the required prediction horizon is 200 ms ahead ( $h = 2$ ). The warm up period is 30 sec, which is 300 samples ( $w = 300$ ). Prediction errors and jitters are reported as averages from observation 301 until the end of the treatment session. We first test the prediction methods stand alone, and then test a selected prediction method inside the proposed algorithm.

All the experiments are performed using in-house produced MATLAB® code, available at <http://datasets.bpti.lt/radiotherapy>.

## **3. Results**

Our experimental analysis consists of two parts: firstly, we experimentally evaluate the performance of alternative prediction methods in terms of prediction error and jitter, and secondly, we experimentally analyze the performance of the proposed algorithmic solution.

### *3.1. Predictive performance of base models*

Figure 4 depicts prediction errors and jitters of the base models, selected in Section 2.4. On the left plot each dot is one time series (recall that each dataset includes three positions, that is, three time series). We can see from the left plot that the selected models provide a variety of errors and jitters, indicating that some of the signals are more difficult to predict than the others. However, dots of the same color (the same base model) appear in elongated clusters, suggesting that there may be a trade-off between error and jitter achieved by different

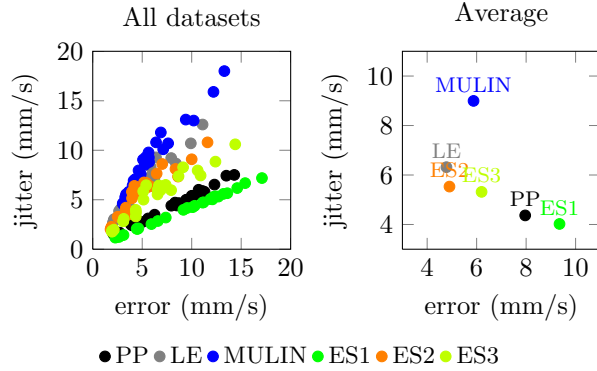


Figure 4: Predictive performance of alternative base models. (left) Each dot is one time series, (right) average performance.

models, that is, a gain in error increases jitter and the other way around. Some models may be better at minimizing error, others at keeping the jitter low. The right plot presents the average overall time series for each model. We see that ES1, PP, ES3 and LE demonstrate nearly a linear trade-off between jitter and error with ES1 showing the lowest jitter and LE showing the lowest error. MULIN demonstrates a reasonable error, but the jitter is much worse than that of the other models. ES2 achieves nearly the same error as LE, but has a lower jitter, therefore, we select ES2 as the primary base model for our algorithmic solution. The performance of a constant prediction, which achieves zero jitter, is not plotted since the error (51mm/s) is too far off the scale of the plot.

### 3.2. Visual analysis

Figure 5 plots the predictions of the compared methods on a snapshot of the first coordinate from the experiment 201205181211-UAC-1-N-320-6. We can see that PP and ES1 have a regular delay in predictions, LE and ES2 overshoot at peaks, MULIN and ES3 follow the signal reasonably well, but MULIN is too spiky (high jitter) and ES3 occasionally makes sudden errors. Based on this visual analysis ES2 or LE are preferred methods. Figure 6 compares the jitters produced by different methods. Each line shows how much the beam would need to travel in 10 seconds if the predictions were followed. We see that



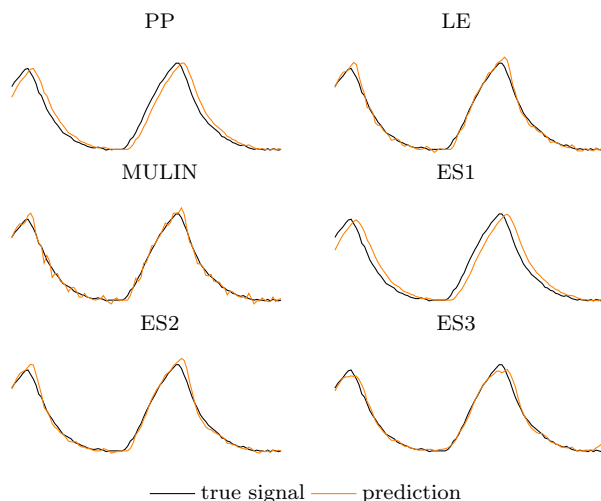


Figure 5: Performance on a snapshot of experiment 201205181211-UAC-1-N-320-6.

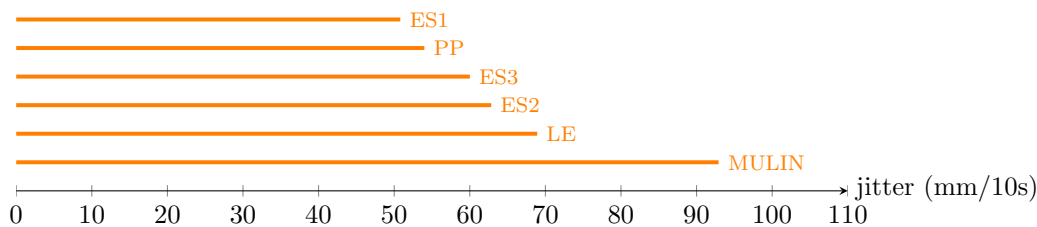


Figure 6: How much the couch would need to travel in 10 s if the predicted signals are followed (including both jitter, and respiratory motion), averaged over experiment 201205181211-UAC-1-N-320-6.

all methods are comparable in terms of jitter except for MULIN, which produces substantially larger jitter.

Next we look at the scatter of predictions in space from a patient’s perspective. Assuming that the bed can perfectly track the predictions, we plot where the beam will hit in 2D with respect to the true target. For that we subtract the true signal from the prediction, this way the true target is always  $(0,0)$ . Intuitively, in order not to cause unnecessary harm to the patient, deviations of predictions from the target  $(0,0)$  should be as small as possible and there should be no far outliers. Moreover, the errors should be distributed around the

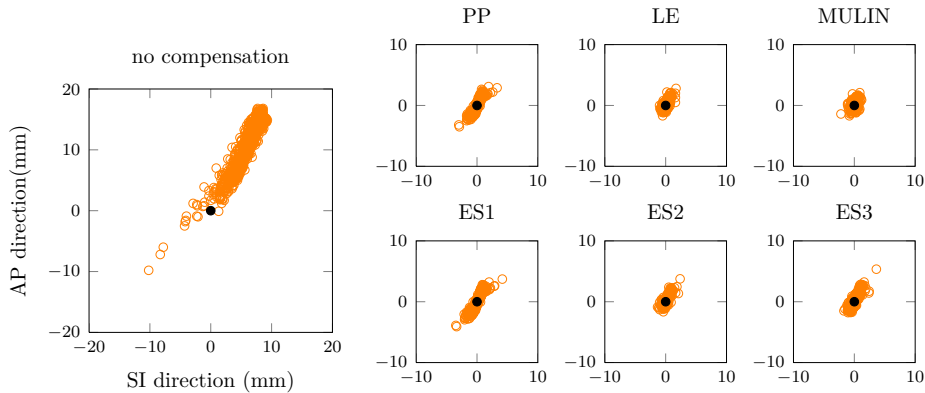


Figure 7: Scatters of predictions on the testing range of 201205181211-UAC-1-N-320-6.

target  $(0, 0)$  as evenly as possible, not concentrated in one or a few spots.

Fig. 7 plots the scatters of predictions for the same experiment 201205181211-UAC-1-N-320-6 (resampled 201205181211-UAC-1-N-320) in 2D (x and z coordinates). We see that all the six methods produce predictions that are reasonably close to the true target, as compared to no compensation. However, PP and LE1 have the strongest tendency to make concentrated errors, meaning that particular two spots on the upper right and lower left sides from the target may be burned due to prediction latency. We would like to notice that in this research tumor is treated as a point (centroid) representing a 3D volume.

### 3.3. Performance of the proposed algorithm

We investigate the performance of EXSMI algorithm with the second order exponential smoothing EXSMI(ES2), which showed the most promising performance in the previous experiment. We compare the performance of the algorithm EXSMI(ES2) with applying ES2 and a naive persistent prediction PP stand alone. Figure 8 plots the errors and jitters on all experiments, one dot represents one dataset and the numerical results are provided in an on-line appendix<sup>8</sup>. We can see from the plot that EXSMI(ES2) has advantage over simple

<sup>8</sup>On-line appendix <http://datasets.bpti.lt/wp-content/uploads/2013/12/ExSmi-OnlineAppendix.pdf>.

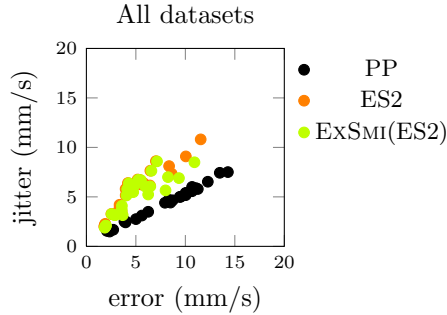


Figure 8: Prediction accuracy.

ES2 in situations where overall error and jitter are quite high, i.e. in extremely unpredictable cases. This performance supports the intuition, that when an intelligent method cannot do well, it makes sense switching to a robust baseline predictor.

Next we analyze this phenomenon in more detail. Table 4 provides average errors and jitters for the experiments divided into two groups: (1) difficult to predict identified by high prediction error ( $> 8$  mm/s) and easy to predict identified by lower prediction error ( $\leq 8$  mm/s). We see that, indeed, for the difficult to predict cases the algorithm provides a better balance between error and jitter, while it does not disturb much the easier to predict cases.

Our dataset includes signals with different activities (such as laughing or talking). Next we analyze the performance of EXSMI at different activities. Table 5 presents the results. We can see that normal position demonstrates the lowest overall error and jitter, as it could be expected, since the patient stays still. Prediction in laughing and talking conditions is, hence, more difficult. The proposed EXSMI performs nearly the same as the base model ES2 in normal/other conditions; however, EXSMI consistently performs the best in other than normal conditions, which is a desired feature of our solution. We have implemented outlier control and predictor switch mechanisms so that the predictions stay robust in difficult situations, and these experimental results support that.

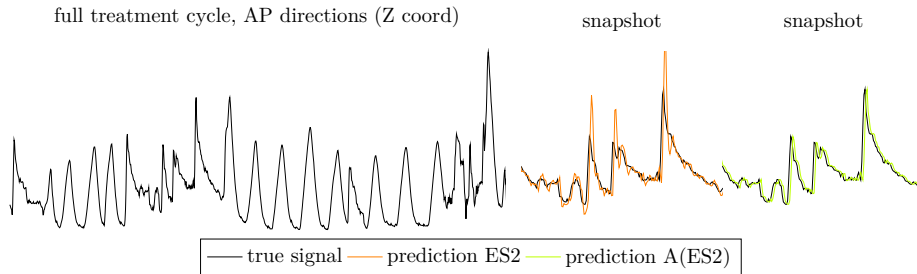


Figure 9: Performance on a snapshot of experiment 201205101536-LAC-1-LT-142-6.

Finally, Figure 9 plots an example of predictions by the algorithm EXSMI(ES2) and ES2 stand alone on a difficult to predict case. We see that when the true signal suddenly starts to jump ES2 largely overshoots. This is because ES2 takes into account the velocity of the signal, observing one sudden jump in the signal level leading to extrapolation of this pattern, i.e. predicting that the signal will jump further with a similar speed. In such a case when the signal is noisy a naive persistent predictor proves to be more accurate. The proposed algorithm combines ES2 and PP and takes advantage of both.

#### 4. Discussion

EXSMI, PP and LE approaches have been implemented in a prototype Rubedo system including a HexaPOD couch, and an infrared stereocamera (NDI Polaris). This prototype validation has confirmed our experimental results, and several additional observations regarding the performance have been made.

1. HexaPOD couch is quite sensitive to larger speed and direction changes and jitter, i.e. the device starts vibrating. Currently, the problem is solved by putting an independent restriction on velocity changes. As a future work, it would be interesting to consider such constraints as part of the prediction algorithm.
2. EXSMI(ES3) implementation seems to be over-sensitive to periodicity changes, while the period of respiratory motion typically is changing all the time.

That explains why the best results have been achieved by EXSMI(ES2) 2 and LE with anti-vibration means.

In this paper only prediction of tumor motion and its compensation is investigated, but in case of external markers motion of tumor should be predicted from a motion of an external marker, e.g. [45, 46], which would induce additional error. This technique requires fixing markers near tumor. However they should be out of the beams' way. The couch used in the setup is not constructed to compensate motion, therefore it is not clear how long and how well it would operate over the extended period of time in such a mode.

Experiments were performed on motion recorded using external markers under an assumption that tumors move in a similar fashion. Therefore, further investigation with tumor motion could be useful.

The important question, which we did not answer in this paper, is how much would a prediction would correct a clinical misalignment of the target? It could be, that linac, MLC, immobilization devices and, especially, a live patient are contribute more the the overall error, while precisions of the most of the existing predictors is sufficient. It is out of scope of this paper, but such analysis could be very interesting.

In summary, the prototype implementation has demonstrated a promising performance, confirmed our experimental findings, and indicated an interesting direction for future investigation.

## 5. Conclusions

The study investigated prediction models and developed an algorithmic solution EXSMI for predicting the position of a target in 3D in real time. EXSMI demonstrated good performance, measured by the prediction accuracy and the jitter of the prediction signal. The developed algorithmic solution performs well to be prototyped deployed in radiation therapy applications.

This study has opened several interesting and important directions for future research. The first direction is to extend the algorithmic solution EXSMI

to take into account technical characteristics of the equipment, for instance, the maximum possible velocity change of the treatment couch. While this study treated each respiratory signal as an independent observation, the second interesting and important direction for extension would be to consider multiple signals from different locations simultaneously. Taking into account such characteristics it is expected to further improve the precision of treatment.

*Conflicts of interest.* Tomas Krilavičius, Indrė Žliobaitė, Henrikas Simonavičius, and Laimonas Jaruševičius declare that they have no conflict of interest.

*Acknowledgements.* We thank Gabrieliūs Čaplinskas, Aušra Vidugirienė and Julius Ruseckas for valuable comments on different aspects of the system. Research was partially funded by ESFA (DADA, VP1-3.1-MM-10-V-02-025).

## References

## References

- [1] M. J. Murphy, Tracking moving organs in real time, *Seminars in Radiation Oncology* 14 (1) (2004) 91–100.
- [2] P. J. Keall, G. S. Mageras, J. M. Balter, R. S. Emery, K. M. Forster, S. B. Jiang, J. M. Kapatoes, D. A. Low, M. J. Murphy, B. R. Murray, C. R. Ramsey, M. B. V. Herk, S. S. Vedam, J. W. Wong, E. Yorke, The management of respiratory motion in radiation oncology report of AAPM Task Group 76, *Medical Physics* 33 (10) (2006) 3874–3900.
- [3] G. C. Sharp, S. B. Jiang, S. Shimizu, H. Shirato, Prediction of respiratory tumour motion for real-time image-guided radiotherapy, *Physics in Medicine and Biology* 49 (3) (2004) 425–440.
- [4] I. Buzurovic, K. Huang, Y. Yu, T. K. Podder, A robotic approach to 4D real-time tumor tracking for radiotherapy, *Physics in Medicine and Biology* 56 (5) (2011) 1299–1318.

- [5] D. Ionascu, S. B. Jiang, S. Nishioka, H. Shirato, R. I. Berbeco, Internal-external correlation investigations of respiratory induced motion of lung tumors, *Medical physics* 34 (2007) 3893.
- [6] S. Bhide, C. Nutting, Recent advances in radiotherapy, *BMC Medicine* 8 (25) (2010) 1–5.
- [7] I. Buzurovic, Y. Yu, M. Werner-Wasik, T. Biswas, P. Anne, A. Dicker, T. Podder, Implementation and experimental results of 4d tumor tracking using robotic couch., *Medical physics* 39 (11) (2012) 6957.
- [8] R. H. Abhilash, S. Chauhan, Empirical modeling of renal motion for improved targeting during focused ultrasound surgery, *Comput. Biol. Med.* 43 (4) (2013) 240–247. doi:10.1016/j.compbimed.2012.11.006.  
URL <http://dx.doi.org/10.1016/j.compbimed.2012.11.006>
- [9] R. Abhilash, S. Chauhan, Respiration-induced movement correlation for synchronous noninvasive renal cancer surgery, *Ultrasonics, Ferroelectrics, and Frequency Control*, *IEEE Transactions on* 59 (7) (2012) 1478–1486.
- [10] S. Siva, D. Pham, S. Gill, M. Bressel, K. Dang, T. Devereux, T. Kron, F. Foroudi, An analysis of respiratory induced kidney motion on four-dimensional computed tomography and its implications for stereotactic kidney radiotherapy, *Radiation Oncology* 8 (1) (2013) 248. doi:10.1186/1748-717X-8-248.  
URL <http://www.ro-journal.com/content/8/1/248>
- [11] S. C. Erridge, Y. Seppenwoolde, S. H. Muller, M. van Herk, K. De Jaeger, J. Belderbos, L. J. Boersma, J. V. Lebesque, Portal imaging to assess set-up errors, tumor motion and tumor shrinkage during conformal radiotherapy of non-small cell lung cancer, *Radiotherapy and Oncology* 66 (1) (2003) 75–85.
- [12] ICRU, Prescribing, recording and reporting photon beam therapy, *Tech.*

- Rep. 50, International Commission on Radiation Units and Measurements (1993).
- [13] ICRU, Prescribing, recording and reporting photon beam therapy (supplement to ICRU report 50), Tech. Rep. 62, International Commission on Radiation Units and Measurements (1999).
- [14] F. Ernst, R. Durichen, A. Schlaefer, A. Schweikard, Evaluating and comparing algorithms for respiratory motion prediction, *Physics in Medicine and Biology* 58 (11) (2013) 3911–3929.
- [15] H. D. Kubo, B. C. Hill, Respiration gated radiotherapy treatment: a technical study, *Physics in medicine and biology* 41 (1) (1996) 83.
- [16] H. Shirato, S. Shimizu, T. Shimizu, T. Nishioka, K. Miyasaka, Real-time tumour-tracking radiotherapy, *The Lancet* 353 (9161) (1999) 1331–1332.
- [17] J. W. Wong, M. B. Sharpe, D. A. Jaffray, V. R. Kini, J. M. Robertson, J. S. Stromberg, A. A. Martinez, The use of active breathing control (ABC) to reduce margin for breathing motion, *International Journal of Radiation Oncology Biology Physics* 44 (4) (1999) 911–919.
- [18] J. R. Adler Jr, S. Chang, M. Murphy, J. Doty, P. Geis, S. Hancock, The cyberknife: a frameless robotic system for radiosurgery, *Stereotactic and functional neurosurgery* 69 (1-4) (1998) 124–128.
- [19] D. Ruan, J. A. Fessler, J. M. Balter, Real-time prediction of respiratory motion based on local regression methods, *Physics in Medicine and Biology* 52 (23) (2007) 7137–7152.
- [20] A. Kalet, G. Sandison, H. Wu, R. Schmitz, A state-based probabilistic model for tumor respiratory motion prediction, *Physics in Medicine and Biology* 55 (24) (2010) 7615–7631.
- [21] L. Dietrich, T. Tücking, S. Nill, U. Oelfke, Compensation for respiratory motion by gated radiotherapy: an experimental study, *Physics in medicine and biology* 50 (10) (2005) 2405–2014.



- [22] P. Keall, A. Todor, S. Vedam, C. Bartee, J. Siebers, V. Kini, R. Mohan, On the use of epid-based implanted marker tracking for 4d radiotherapy, *Medical physics* 31 (2004) 3492.
- [23] T. Solberg, P. Medin, E. Ramirez, C. Ding, R. Foster, J. Yordy, Commissioning and initial stereotactic ablative radiotherapy experience with vero, *Journal of Applied Clinical Medical Physics* 15 (2).  
URL <http://www.jacmp.org/index.php/jacmp/article/view/4685>
- [24] Y. Seppenwoolde, R. I. Berbeco, S. Nishioka, H. Shirato, B. Heijmen, Accuracy of tumor motion compensation algorithm from a robotic respiratory tracking system: A simulation study, *Medical Physics* 34 (7) (2007) 2774–2784. doi:<http://dx.doi.org/10.1118/1.2739811>.  
URL <http://scitation.aip.org/content/aapm/journal/medphys/34/7/10.1118/1.2739811>
- [25] Y. Tsunashima, T. Sakae, Y. Shioyama, K. Kagei, T. Terunuma, A. Nohtomi, Y. Akine, Correlation between the respiratory waveform measured using a respiratory sensor and 3D tumor motion in gated radiotherapy, *International Journal of Radiation Oncology Biology Physics* 60 (3) (2004) 951–958.
- [26] A. Schweikard, G. Glosser, M. Bodduluri, M. J. Murphy, J. R. Adler, Robotic motion compensation for respiratory movement during radiosurgery, *Computer Aided Surgery* 5 (4) (2000) 263–277.
- [27] T. Krilavičius, D. Vitkutė-Adžgauskienė, K. Šidlauskas, Simulation of the radiation therapy system for respiratory movement compensation, *Journal of Vibroengineering* 14 (2012) 99–104.
- [28] D. Putra, O. C. Haas, J. A. Mills, K. J. Burnham, A multiple model approach to respiratory motion prediction for real-time IGRT, *Physics in Medicine and Biology* 53 (6) (2008) 1651–1663.

- [29] M. J. Murphy, D. Pokhrel, Optimization of an adaptive neural network to predict breathing, *Medical Physics* 36 (1) (2009) 40–47.
- [30] K. Ichiji, N. Homma, M. Sakai, Y. Narita, Y. Takai, X. Zhang, M. Abe, N. Sugita, M. Yoshizawa, A time-varying seasonal autoregressive model-based prediction of respiratory motion for tumor following radiotherapy, *Computational and Mathematical Methods in Medicine 2013* (2013) Article ID 390325.
- [31] Q. Ren, S. Nishioka, H. Shirato, R. I. Berbeco, Adaptive prediction of respiratory motion for motion compensation radiotherapy, *Physics in Medicine and Biology* 52 (22) (2007) 6651–6661.
- [32] F. Ernst, A. Schweikard, Predicting respiratory motion signals for image-guided radiotherapy using multi-step linear methods (MULIN), *International Journal of Computer Assisted Radiology and Surgery* 3 (1) (2008) 85–90.
- [33] F. Ernst, A. Schlaefer, A. Schweikard, Prediction of respiratory motion with wavelet-based multiscale autoregression, in: *Proc. of the 10th int. conf. on Medical image computing and computer-assisted intervention, MICCAI, 2007*, pp. 668–675.
- [34] O. C. L. Haas, P. Skworcow, D. Paluszczyszyn, A. Sahih, M. Ruta, J. A. Mills, Couch-based motion compensation: modelling, simulation and real-time experiments, *Physics in Medicine and Biology* 57 (18) (2012) 5787–5807.
- [35] C. Herrmann, L. Ma, K. Schilling, Model predictive control for tumor motion compensation in robot assisted radiotherapy, in: *Preprints of the 18th IFAC World Congress, Vol. 18, 2011*, pp. 5968–5973.
- [36] H. Chung, H. Jin, T. Suh, J. Palta, S. Kim, Characterization of a commercial add-on couch, HexaPOD<sup>TM</sup> 6D robotic treatment couchTOP, in:

World Congress on Medical Physics and Biomedical Engineering, Vol. 14 of IFMBE Proceedings, Springer, 2007, pp. 1945–1947.

- [37] J. Meyer, M. Guckenberger, J. Wilbert, K. Baier, On the use of a Hexapod table to improve tumour targeting in radiation therapy, in: M. Habib (Ed.), *Bioinspiration and Robotics Walking and Climbing Robots*, I-Tech Education and Publishing, 2007, pp. 529–544.
- [38] K. L. Man, T. Krilavičius, K. Wan, D. Hughes, K. Lee, Modeling and analysis of radiation therapy system with respiratory compensation using uppaal, *Proc. of the 9th IEEE Int. Symp. on Parallel and Distributed Processing with Applications Workshops (2011)* 50–54.
- [39] T. Krilavičius, K. L. Man, Timed model of the radiation therapy system with respiratory motion compensation, in: *Proc. of the 6th Int. Conf. on Electrical and Control Technologies, ECT*, 2011, pp. 1–4.
- [40] A. D. Wiles, D. G. Thompson, D. D. Frantz, Accuracy assessment and interpretation for optical tracking systems, in: *Proceedings of the SPIE –The International Society for Optical Engineering*, 2004, pp. 421–432.
- [41] G. Box, G. Jenkins, *Time series analysis: Forecasting and control*, San Francisco: Holden-Day, 1970.
- [42] P. Goodwin, The Holt-Winters approach to exponential smoothing: 50 years old and going strong, *Foresight: The International Journal of Applied Forecasting* 19 (2010) 30–33.
- [43] R. J. Hyndman, G. Athanasopoulos, *Forecasting: principles and practice*, OTexts, 2012.
- [44] F. Ernst, A. Schlaefer, A. Schweikard, Predicting the outcome of respiratory motion prediction, *Medical Physics* 38 (2011) 5569–5581.
- [45] T. Krilavičius, R. Užupytė, I. Žliobaitė, H. Simonavičius, Correlation of external markers and functional targets for respiration compensation in

radiotherapy, in: Medical Physics in the Baltic States 11(2013), 2013, pp. 42–45.

- [46] R. Užupytė, K. Man, T. Krilavičius, I. Žliobaitė, H. Simonavičius, Indirect tracking of functional target for respiration compensation in radiotherapy, in: Proc. of The International MultiConference of Engineers and Computer Scientists (IMECS), 2015, pp. 733–736.

### **Appendix A. Jitter per time spacing and relative error**

Table A.6 presents jitter and error of Figure 4 relative to PP.

Table A.7 presents jitter and error of Table 4 relative to PP.

Table 1: Experimental Data, where SI (superior-inferior) positions are (L-lower, U-upper), body positions (A-abdomen, C-chest and LR (L-left, C-center, R-right)), and different states (T-talking, N-normal, O-other (other type of motion), L-laughing); directions: SI (superior-inferior), LR (left-right), AP (anterior-posterior)

Signals	Max Range SI, LR, AP (mm)	Duration (s)	Frames	Experimental setting
201205101519- LACUACUCC-3- T-222	19, 4, 23	222.00	6658	lower abdomen center, upper abdomen center, upper chest center, talking
201205101522- LACUACUCC-3- N-138	6, 3, 20	138.00	4148	lower abdomen center, upper abdomen center, upper chest center, normal
201205101534- LACUACUCC-3- NO-130	9, 4, 20	130.00	3883	lower abdomen center, upper abdomen center, upper chest center, normal, other
201205101536- LACUACUCC-3- LT-142	29, 14, 31	142.00	4267	lower abdomen center, upper abdomen center, upper chest center, laughing, talking
201205101541- LACUACUCC-3- N-130	6, 2, 17	131.00	3919	lower abdomen center, upper abdomen center, upper chest center, normal
201205111055- LAFLARUAR-3- N-117	6, 4, 18	117.00	3513	lower abdomen center, lower abdomen right, upper abdomen right, normal
201205111057- LAFLARUAR-3- O-72	40, 10, 45	72.62	2178	lower abdomen center, lower abdomen right, upper abdomen right, other
201205181211- LACUACUCC-3- N-320	12, 4, 31	320.05	9593	lower abdomen center, upper abdomen center, upper chest center, normal
201205181220- LACUACUCC-3- N-306	20, 5, 36	306.00	9176	lower abdomen center, upper abdomen center, upper chest center, normal

Table 2: Qualitative assessment and selection of base models.

Technique	Fast to calibrate	Adaptive	Transparent	Simple to implement	Select
Extrapolation methods	yes	yes	yes	yes	✓
Exponential smoothing	yes	yes	yes	yes	✓
State-based probabilistic	no	yes/no	yes	yes	
Autoregressive models	no	yes/no	yes	yes/no	
Neural networks	no	yes/no	no	no	
Support vector machines	no	no	no	no	

Table 3: Recommended parameters for exponential smoothing.

Model	level	trend	seasonal	respiratory rate
	$\alpha$	$\beta$	$\gamma$	$p$
ES1	0.7			
ES2	0.7	0.6		
ES3	0.7	0.3	0.3	5.5 sec

Table 4: Average performance on difficult and easy to predict cases.

Group	Measure (mm)	$PP$	$ES2$	$ExSMI(ES2)$	
Difficult	average error	10.8	9.6	9.1	
	$E$	(std.)	(2.1)	(1.5)	(1.3)
	>	average jitter	6.0	8.8	7.0
	8 mm/s	(std.)	(1.1)	(1.5)	(1.2)
		error + jitter	16.8	18.4	16.1
Easy	average error	7.5	4.1	4.2	
	$E$	(std.)	(3.7)	(1.6)	(1.6)
	$\leq$	average jitter	4.1	5.0	4.8
	8 mm/s	(std.)	(1.8)	(1.9)	(2.0)
		error + jitter	11.5	9.0	9.0

ALGORITHM 1: Predict respiratory signal  $h$  steps ahead

```

1: incoming observations  $r = (x, y, z)$ 
2: predictive model form  $L$  with design parameters  $\theta$ 
3: prediction horizon  $h$ , warm-up  $w$  (recommended  $w \sim 30$  s)
4: decay for measuring recent error  $d \in (0, 1)$  (rec.  $d = 0.1$ )
5: Initialize model  $L_0$  (See Sec. 2.4 for recommendations)
6: Initialize error and jitter counts  $E_0^L = 0, E_0^B = 0, J^L = 0, J^B = 0$ 
7: for  $t \leftarrow 2, \dots, I$  do /*from the start to the end of treatment*/
8:   receive the latest observation  $r_t$ 
9:   if  $\|r_t - r_{t-1}\| < 1$  cm then
10:    update model  $L_t = f(L_{t-1}, (x, y, z)_t)$ 
11:    if  $t < w$  then /*if warmup is over make predictions*/
12:      make prediction with  $L_t$ :  $\hat{r}_{t+h}^L$ 
13:      make baseline prediction  $\hat{r}_{t+h}^B = r_t + (r_t - r_{t-h})$ 
14:      error  $E_t^L = d * \text{error}(\hat{r}_t, r_t) + (1 - d)E_{t-1}^L$  [Eq. (1)]
15:      error  $E_t^B = d * \text{error}(r_{t-h}, r_t) + (1 - d)E_{t-1}^B$  [Eq. (1)]
16:      jitter  $J_t^L = d * \text{jitter}(\hat{r}_t, \hat{r}_{t-1}) + (1 - d)J_{t-1}^L$  [Eq. (3)]
17:      jitter  $J_t^B = d * \text{jitter}(r_{t-h}, r_{t-h-1}) + (1 - d)J_{t-1}^B$  [Eq. (3)]
18:      if  $(E_t^L + J_t^L) > (E_t^B + J_t^B)$  then /*L performs well*/
19:        final prediction by the main model  $\hat{r}_{t+h} = \hat{r}_{t+h}^L$ 
20:      else
21:        final prediction by baseline  $\hat{r}_{t+h} = \hat{r}_{t+h}^B$ 
22:      end if
23:    end if
24:    else /* $r_t$  is an outlier, ignore*/
25:      if  $t < w$  then
26:        predict  $\hat{r}_{t+h} = \hat{r}_{t+h-1}$ 
27:        set  $E_t^L = E_{t-1}^L, E_t^B = E_{t-1}^B, J_t^L = J_{t-1}^L, J_t^B = J_{t-1}^B$ 
28:      end if
29:    end if
30:    adjust the beamer /*out of the scope of this paper*/
31:  end for

```

Table 5: Average performance with different activities.

<b>Group</b>	<b>Measure (mm/s)</b>	<i>PP</i>	<i>ES2</i>	EXSMI( <i>ES2</i> )
Normal	average error	7.0	3.9	4.0
	average jitter	3.9	4.7	4.6
	error + jitter	10.9	8.6	8.6
Normal/ other	average error	8.1	4.0	4.0
	average jitter	4.2	5.0	5.0
	error + jitter	12.3	9.0	9.0
Talking	average error	10.2	4.6	4.8
	average jitter	5.3	6.2	6.1
	error + jitter	15.6	10.8	10.9
Talking	average error	7.6	6.1	6.1
	average jitter	4.2	5.9	5.1
	error + jitter	11.8	12.0	11.2
Laughing/ talking	average error	10.8	10.1	9.4
	average jitter	6.0	9.1	7.0
	error + jitter	16.8	19.2	16.4

Table A.6: Predictive performance of the base models relative to persistent prediction (PP).

	PP	LE	MULIN	ES1	ES2	ES3
relative error	1.00	0.60	0.74	1.17	0.62	0.78
relative jitter	1.00	1.45	2.06	0.92	1.27	1.22



Table A.7: Relative performance on difficult to predict and easy to predict cases.

	Measure	PP	ES2	EXSMI(ES2)
Difficult	relative error	1.00	0.89	0.84
$E > 8$	relative jitter	1.00	1.47	1.17
mm/s	error + jitter	1.00	1.09	0.96
Easy	relative error	1.00	0.55	0.56
$E \leq 8$	relative jitter	1.00	1.21	1.18
mm/s	error + jitter	1.00	0.78	0.78